Observation of the Electromagnetic Radiative Decays of the $\Lambda(1520)$ and $\Lambda(1690)$ to $\gamma\Sigma^0$

M. Ablikim *et al.*[*]
(BESIII Collaboration)

(Received 16 July 2025; revised 16 February 2026; accepted 3 March 2026; published 8 April 2026)

Using $(10087 \pm 44) \times 10^6$ J/ψ events collected with the BESIII detector, we present a study of resonant structures in the $J/\psi \to \Lambda\bar{\Lambda}\gamma$ and $\Lambda\bar{\Sigma}^0\gamma$ processes, reporting the first observation of the electromagnetic radiative decays of the $\Lambda(1520)$ and $\Lambda(1690)$ to $\gamma\Sigma^0$, with a statistical significance of 16.6σ and 23.2σ, respectively. The ratio of the branching fractions $\{\mathcal{B}[\Lambda(1520) \to \gamma\Lambda]/\mathcal{B}[\Lambda(1520) \to \gamma\Sigma^0]\}$ is determined to be $3.19 \pm 0.34(\text{stat}) \pm 0.19(\text{syst})$, which is in agreement with flavor SU(3) symmetry within two standard deviations. The branching fraction of $\Lambda(1520) \to \gamma\Sigma^0$ is measured to be $\mathcal{B}[\Lambda(1520) \to \gamma\Sigma^0] = [2.66 \pm 0.28(\text{stat}) \pm 0.50(\text{syst})] \times 10^{-3}$, corresponding to a partial width of $\Gamma[\Lambda(1520) \to \gamma\Sigma^0] = [46.8 \pm 6.6(\text{stat}) \pm 9.3(\text{syst})]$ keV, which is inconsistent with predictions from the relativized constituent quark model and the Algebraic model. Additionally, we observe a clear resonant structure in the $\gamma\Sigma^0$ mass spectrum near 1.7 GeV/c^2, attributed to the $\Lambda(1690)$. The product branching fraction $\mathcal{B}[J/\psi \to \bar{\Lambda}\Lambda(1690) + \text{c.c.}] \times \mathcal{B}[\Lambda(1690) \to \gamma\Sigma^0]$ is measured for the first time as $[6.05 \pm 0.42(\text{stat}) \pm 0.39(\text{syst})] \times 10^{-6}$. However, no corresponding structure is seen in the $\gamma\Lambda$ mass spectrum, so an upper limit on the product branching fraction $\mathcal{B}[J/\psi \to \bar{\Lambda}\Lambda(1690) + \text{c.c.}] \times \mathcal{B}[\Lambda(1690) \to \gamma\Lambda]$ is determined to be 5.08×10^{-7} at the 90% confidence level.

DOI: 10.1103/l6g2-2wg6

The emitted photon in hyperon radiative decay carries information about the properties of the initial and final hyperon states, making it a unique probe for exploring the underlying quark structure and interactions within hyperons. This has attracted attention from both experimental and theoretical perspectives. While the importance of these decays has been stressed for over half a century, it has remained a significant challenge to find a consistent picture between the theoretical descriptions and the experimental results for hyperon radiative decays.

Some different theoretical approaches [1–4], at both the baryon and quark levels, have been employed to investigate hyperon radiative decays, and significant theoretical progress has been made. However, a completely satisfactory description is still lacking. The experimental situation has improved significantly over the past few years with the advent of the BESIII experiment. Taking advantage of the high production rate of hyperons in J/ψ decays, several radiative hyperon decays, in particular for the octet ground states, have been measured by BESIII for the first time [5,6].

However, experimental results for radiative decays of excited hyperons are still very sparse. Even for the narrow $\Lambda(1520)$, the most recent data on $\Lambda(1520) \to \gamma\Lambda$ dates back twenty years [7], and the decay $\Lambda(1520) \to \gamma\Sigma^0$ has not yet been observed. These decays are of particular interest as they offer further insight into the internal structure of the $\Lambda(1520)$, which has inspired considerable theoretical speculation. Assuming it is a flavor SU(3) singlet, the predicted ratio of decay widths between $\Lambda(1520) \to \gamma\Lambda$ and $\Lambda(1520) \to \gamma\Sigma^0$ is approximately 2.5 [8]. Theoretical predictions from models such as the χQM, non-relativistic quark model (NRQM), relativistic constituent quark model (RCQM), MIT Bag, Chiral Bag, and Algebraic models, as summarized in Table I, show significant variations in the expected rates for these two processes.

TABLE I. Theoretical predictions and experimental measurements of the partial widths of $\Lambda(1520) \to \gamma\Lambda$ and $\Lambda(1520) \to \gamma\Sigma^0$ (in keV).

Decay	$\Lambda(1520) \to \gamma\Lambda$	$\Lambda(1520) \to \gamma\Sigma^0$
χQM [4]	134	92
NRQM	156 [9], 96 [10]	55 [9], 74 [10]
RCQM [11]	215	293
MIT bag [9]	46	17
Chiral bag [12]	32	49
Algebraic model [13]	85.1	180.4
CLAS Collaboration [7]	$167 \pm 43^{+26}_{-12}$	⋯

[*]Full author list given at the end of the Letter.

Published by the American Physical Society under the terms of the Creative Commons Attribution 4.0 International license. Further distribution of this work must maintain attribution to the author(s) and the published article's title, journal citation, and DOI. Funded by SCOAP[3].

Therefore, more precise measurements of the branching fractions of these excited hyperon decays not only are crucial for validating theoretical models but also provide valuable insights into the interactions among confined light quarks.

In this Letter, through a study of resonant structures in the $J/\psi \to \Lambda\bar{\Lambda}\gamma$ and $\Lambda\bar{\Sigma}^0\gamma$ processes, we report the first observation of the electromagnetic radiative transition $\Lambda(1520) \to \gamma\Sigma^0$ with a sample of $(10087 \pm 44) \times 10^6$ J/ψ events [14]. The measurement of the ratio $\{\mathcal{B}[\Lambda(1520) \to \gamma\Lambda]/\mathcal{B}[\Lambda(1520) \to \gamma\Sigma^0]\}$, along with the corresponding partial width of $\Lambda(1520)$, is also presented. In addition, a clear resonant peak near 1.7 GeV/c^2, which is attributed to the $\Lambda(1690)$, in the $\gamma\Sigma^0$ mass spectrum is observed for the first time, but no evident signal of $\Lambda(1690) \to \gamma\Lambda$ is seen. The inclusion of charge-conjugate processes is implied.

The design and performance of the BESIII detector are described in detail in Refs. [15,16]. Simulated samples, including both inclusive and exclusive events produced with the GEANT4-based [17] Monte Carlo (MC) package, which encompasses the geometric description of the BESIII detector and its response, are utilized to determine the detection efficiency and estimate backgrounds. The processes $J/\psi \to \bar{\Lambda}\Lambda(1520/1690)$ and the subsequent electromagnetic transitions $\Lambda(1520/1690) \to \gamma\Lambda(\Sigma^0)$ are simulated using the phase space model implemented in the EVTGEN MC event generator [18,19].

In the analysis of both $\Lambda(1520/1690) \to \gamma\Lambda$ (Mode I) and $\Lambda(1520/1690) \to \gamma\Sigma^0$ (Mode II), the Σ^0 and Λ are reconstructed with their decay modes of $\Sigma^0 \to \gamma\Lambda(\Lambda \to p\pi^-)$ and $\Lambda \to p\pi^-$, respectively. The candidate charged tracks and electromagnetic showers are required to satisfy the following common selection criteria. (i) Charged tracks are reconstructed using the tracking information from the multilayer drift chamber (MDC). The distance of closest approach of each charged track to the e^+e^- interaction point is required to be within ± 20 cm along the beam direction and within 10 cm in the plane perpendicular to the beam direction. The polar angle θ between the direction of a charged track and that of the beam must satisfy $|\cos\theta| < 0.93$ for an effective measurement in the active volume of the MDC. (ii) Electromagnetic showers are reconstructed from clusters of deposited energy in the electromagnetic calorimeter (EMC). The shower energies of photon candidates must exceed 25 MeV in the barrel region ($|\cos\theta| < 0.80$) or 50 MeV in the end cap regions ($0.86 < |\cos\theta| < 0.92$). Showers located in the transition regions between the barrel and the end cap regions are excluded. To avoid showers caused by charged particles, a photon candidate has to be separated by at least 10° from any charged track. To suppress electronic noise and unrelated energy deposits, the EMC time t of the photon candidates must fall within the range $0 \le t \le 700$ ns. (iii) To reconstruct the decays $\Lambda \to p\pi^-$ and $\bar{\Lambda} \to \bar{p}\pi^+$, we loop over all combinations of positive and negative charged track pairs and require that at least one $(p\pi^-)(\bar{p}\pi^+)$ track hypothesis successfully passes the vertex finding algorithm [20] of Λ and $\bar{\Lambda}$. If multiple $p\pi^-$ combinations satisfy the vertex fit requirement, the one with the mass closest to M_Λ is chosen, where M_Λ is the nominal mass of Λ [21]. The $p\pi^-$ and $\bar{p}\pi^+$ pairs are accepted as Λ and $\bar{\Lambda}$ candidates if their invariant masses satisfy $|M_{p\pi^-} - M_\Lambda| < 5$ MeV/c^2 and $|M_{\bar{p}\pi^+} - M_\Lambda| < 5$ MeV/c^2, respectively.

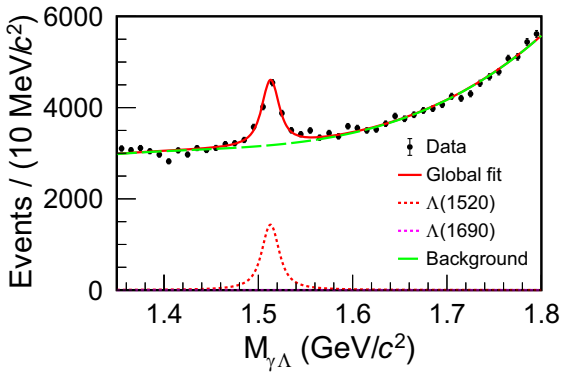


FIG. 1. Fit result of $M(\gamma\Lambda)$. The black dots with error bars are data, the red curve is the global fit, the red dotted-curve is the $\Lambda(1520)$ signal, the pink long-dashed curve is the $\Lambda(1690)$ signal, and the green long-dashed curve is the fitted background shape. No $\Lambda(1690)$ signal is apparent.

For Mode I, to further suppress backgrounds and improve mass resolution, a four-constraint energy momentum conservation (4C) kinematic fit is performed with the hypothesis of $\gamma\Lambda\bar{\Lambda}$. The 4C kinematic fit, by constraining the total four momentum of the final-state particles to the known initial J/ψ four momentum, effectively performs a global event reconstruction, providing powerful suppression of backgrounds. Events with the chi-square value from the four-constraint kinematic fit $\chi^2_{\rm 4C} < 30$ are retained. In addition, $|M_{\gamma\bar{\Lambda}} - M_{\Sigma^0}| > 0.02$ GeV/c^2 and $|M_{\gamma\Lambda} - M_{\Sigma^0}| > 0.02$ GeV/c^2 are required in the further analysis for $J/\psi \to \bar{\Lambda}\Lambda(1520)$ and $J/\psi \to \Lambda\bar{\Lambda}(1520)$, respectively, which effectively suppresses the $J/\psi \to \bar{\Lambda}\Sigma^0$ background. Following these requirements, the invariant mass spectrum of $\gamma\Lambda$ is displayed in Fig. 1, where the prominent peak of $\Lambda(1520)$ is clearly observed while there is no significant $\Lambda(1690)$ signal. Potential background events are investigated using an inclusive MC sample of 10 billion J/ψ events generated with the EVTGEN [18,19] and LUNDCHARM [22,23]. Employing the same selection criteria and a topology study, it is indicated that the main background originates from $J/\psi \to \gamma\Lambda\bar{\Lambda}$, with no evident peak in the $\Lambda(1520/1690)$ mass region. Further data-driven sideband analysis is provided in Supplemental Material [24].

For Mode II, a 4C kinematic fit is performed under the hypothesis of $\gamma\gamma\Lambda\bar{\Lambda}$, retaining those events with $\chi^2_{\rm 4C} < 15$.

To effectively suppress background events from $J/\psi \to \bar{\Lambda}\Sigma^0\pi^0$, we implement a sequential analysis procedure involving kinematic fits and selection criteria. First, a one-constraint (1C) kinematic fit is applied to the $\gamma\Lambda$ hypothesis with the invariant mass constrained to the Σ^0 nominal mass, enabling extraction of the $\bar{\Lambda}\Sigma^0$ squared recoil mass $(M^{\rm rec}_{\bar{\Lambda}\Sigma^0})^2$ and significantly reducing this background. Subsequently, a two-constraint (2C) kinematic fit is performed on the complete $\gamma, \pi^0(\to \gamma\gamma_{\rm miss}), \Lambda, \bar{\Lambda}$ hypothesis, incorporating energy-momentum conservation and requiring the $\gamma\gamma_{\rm miss}$ system to match the π^0 mass. The combined application of selection criteria $(M^{\rm rec}_{\bar{\Lambda}\Sigma^0})^2 < 0.01\ ({\rm GeV}/c^2)^2$ and $\chi^2_{\rm 2C} > 5$ provides additional background suppression, substantially enhancing the purity of the signal events through this two-stage approach. To suppress background events with π^0 in the final state, we require $|M_{\gamma\gamma} - M_{\pi^0}| > 0.03\ {\rm GeV}/c^2$. The events with both $\gamma\Lambda$ and $\gamma\bar{\Lambda}$ in the Σ^0 mass regions are rejected for the background events from $J/\psi \to \Sigma^0\bar{\Sigma}^0$. Since the photon from $\Lambda(1520/1690)$ generally has higher energy than that from Σ^0 decay, the lower-energy photon is assumed to originate from Σ^0, and a requirement of $|M_{\gamma_{\rm low}\Lambda} - M_{\Sigma^0}| < 0.01\ {\rm GeV}/c^2$ is applied to select the Σ^0 signal. After these requirements, the invariant mass spectrum of $\gamma\Sigma^0$ is presented in Fig. 2, where the prominent peaks of $\Lambda(1520)$ and $\Lambda(1690)$ are clearly observed. Possible background sources are investigated with an inclusive MC sample of 10 billion J/ψ events. Employing the same selection criteria, it is indicated that the main background originates from $J/\psi \to \gamma\bar{\Lambda}\Sigma^0$, with no peaking structure observed in the $\Lambda(1520/1690)$ signal region. The sideband analysis is provided in Supplemental Material [24].

The signal yields of the exclusive channels are derived from simultaneous unbinned maximum likelihood fits applied to the mass spectra of selected candidates for $\Lambda(1520/1690) \to \gamma\Lambda$ and $\Lambda(1520/1690) \to \gamma\Sigma^0$. In these fits, the signal components are modeled using Breit-Wigner convoluted with a fixed Gaussian function determined from the MC study to account for the resolution of the reconstruction. The background is represented by the third-order and second-order Chebyshev polynomial functions for Mode I and Mode II, respectively, with free background yield. The fits, as illustrated in Figs. 1 and 2, yield 4043 ± 247 events for $\Lambda(1520) \to \gamma\Lambda$ and 621 ± 53 events for $\Lambda(1520) \to \gamma\Sigma^0$ with a statistical significance of 16.6σ. The statistical significance is determined by the change of the log-likelihood value and the number of degrees of freedom in the fit with and without the $\Lambda(1520)$ signal. The extracted width of (17.6 ± 1.6) MeV is consistent with the world average value of $\Lambda(1520)$ [21], and the fitted mass of $(1515.4 \pm 0.5)\ {\rm MeV}/c^2$ is lower than the world average. This discrepancy is due to the asymmetric line shape arising from interference between the $\Lambda(1520)$ resonance and the nonresonant background, which is considered a source of systematic uncertainty in the mass extraction. Furthermore, the $\Lambda(1690) \to \gamma\Sigma^0$ signal is observed with 1754 ± 122 events with a statistical significance of 23.2σ evaluated using the same method as for $\Lambda(1520)$, from which a mass of $(1683.9 \pm 1.3)\ {\rm MeV}/c^2$ and a width of (48.8 ± 4.0) MeV are obtained. Although the Particle Data Group lists nearby states such as the $\Lambda(1670)$ and $\Sigma(1670)$ with different quantum numbers, the measured mass and width are more consistent with the world averages for the $\Lambda(1690)$ than with those of the $\Lambda(1670)$. Furthermore, the production mechanism $J/\psi \to \bar{\Lambda}\Lambda(1690)$ favors an isoscalar hyperon, providing additional support for this assignment. Conversely, interpretation as the isovector $\Sigma(1670)$ is highly suppressed in J/ψ decays due to isospin conservation. Additional analysis of angular distributions, detailed in Supplemental Material [24], quantitatively favors the $J^P = 3/2^-$ assignment for the peak near 1.7 ${\rm GeV}/c^2$ over the $J^P = 1/2^-$ hypothesis. The goodness-of-fit, expressed as χ^2 per degree of freedom (NDF), favors the $\Lambda(1690)$ hypothesis ($\chi^2/{\rm NDF} = 2.5$) over the $\Lambda(1670)$ hypothesis ($\chi^2/{\rm NDF} = 4.3$), further supporting its identification as the $\Lambda(1690)$.

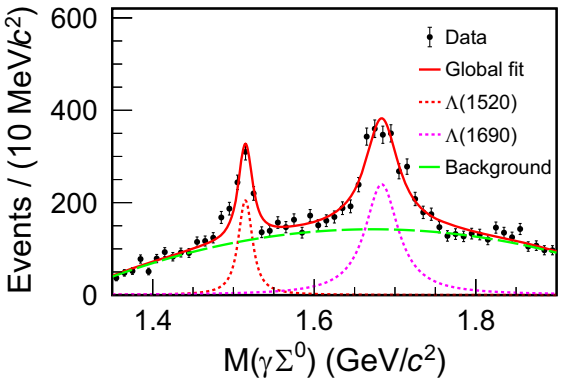


FIG. 2. Fit result of $M(\gamma\Sigma^0)$. The black dots with error bars are data, the red curve is the global fit, the red dotted-curve is the $\Lambda(1520)$ signal, the pink long-dashed curve is the $\Lambda(1690)$ signal and the green long-dashed curve is from the fitted background shape.

With the detection efficiencies obtained from the MC simulations, the ratio of the branching fractions is calculated with

$$\mathcal{R} = \frac{\mathcal{B}[\Lambda(1520/1690) \to \gamma\Lambda]}{\mathcal{B}[\Lambda(1520/1690) \to \gamma\Sigma^0]} = \frac{N^{\rm obs}_{\gamma\Lambda}}{N^{\rm obs}_{\gamma\Sigma^0}} \cdot \frac{\epsilon_{\gamma\Sigma^0}}{\epsilon_{\gamma\Lambda}}, \quad (1)$$

where $N^{\rm obs}_{\gamma\Lambda}$ and $N^{\rm obs}_{\gamma\Sigma^0}$ are the signal yields (or the upper limit at the 90% confidence level) and $\epsilon_{\gamma\Sigma^0}$ and $\epsilon_{\gamma\Lambda}$ are the corresponding detection efficiencies. With the numbers given in Table II, $\mathcal{R}$ for $\Lambda(1520)$ decay is determined to be 3.19 ± 0.34, where the uncertainty is statistical only. The product branching fraction is calculated with

TABLE II. Signal yields, detection efficiencies, and the $\mathcal{R}$ of each signal decay. The first uncertainties are statistical, and the second uncertainties are systematic.

Decay	$N^{\rm obs}$	$\epsilon_{\gamma\Lambda/\gamma\Sigma^0}$	$\mathcal{R}$
$\Lambda(1520)\to\gamma\Lambda$	4043 ± 247	18.91%	$3.19\pm0.34\pm0.19$
$\Lambda(1520)\to\gamma\Sigma^0$	621 ± 53	9.28%	
$\Lambda(1690)\to\gamma\Lambda$	<341	16.20%	<0.08
$\Lambda(1690)\to\gamma\Sigma^0$	1754 ± 122	7.00%	

$$\mathcal{B}[J/\psi\to\bar{\Lambda}\Lambda(1690)]\times\mathcal{B}[\Lambda(1690)\to\gamma\Lambda(\Sigma^0)] = \frac{N^{\rm obs}_{\gamma\Sigma^0}}{N_{J/\psi}\times\mathcal{B}^2(\Lambda\to p\pi)\times\epsilon_{\gamma\Sigma^0}}, \quad (2)$$

where $N_{J/\psi}$ is the total number of J/ψ events and world average $\mathcal{B}(\Lambda\to p\pi)$ [21] is used. With the numbers given in Table II, $\mathcal{B}[J/\psi\to\bar{\Lambda}\Lambda(1690)]\times\mathcal{B}[\Lambda(1690)\to\gamma\Sigma^0]$ is determined to be $(6.05\pm0.42)\times10^{-6}$, where the uncertainty is statistical only.

Since no significant signal is evident for the decay $\Lambda(1690)\to\gamma\Lambda$, as illustrated in Fig. 1, we set the upper limit on the signal yield at the 90% confidence level with the Bayesian approach [25]. In order to determine the likelihood distribution, a series of unbinned extended maximum likelihood fits are performed to the mass spectrum of $\gamma\Lambda$ scanning along the magnitude of the $\Lambda(1690)$ signal. In the fit, the line shape of the $\Lambda(1690)$ signal is determined by Breit-Wigner convoluted with a fixed Gaussian resolution function determined from the MC study, and the background is represented with a third-order Chebychev polynomial function. The resultant likelihood distribution is taken as the probability density function directly. The upper limit on the number of signal events at the 90% confidence level is defined as $N_{\rm UL}$, corresponding to the number of events at 90% of the integral of the probability density function of likelihood distribution. To account for the additive systematic uncertainties from the mass spectrum fit, the alternative fits are performed with different fit ranges and background shapes and the maximum one, $N_{\rm UL}=339$, is used to evaluate the upper limit on the branching fraction of the decay of interest.

The final upper limit on the product branching fraction also considers the multiplicative systematic uncertainty, which is accounted for by convolving the likelihood distribution $\mathcal{L}(N)$ to obtain the smeared likelihood $\mathcal{L}'(N)$,

$$\mathcal{L}'(N)=\int_0^1\mathcal{L}\left(\frac{S}{\hat{S}}N\right)\exp\left[-\frac{(S-\hat{S})}{2\sigma_S^2}\right]dS. \quad (3)$$

In this expression $\hat{S}$ is the nominal efficiency, and σ_S is its absolute systematic uncertainty. Following this procedure, the upper limit on the number of $\Lambda(1690)\to\gamma\Lambda$ signal events at the 90% confidence level is set to be 341, and the corresponding upper limit of the product branching fraction is $\mathcal{B}[J/\psi\to\bar{\Lambda}\Lambda(1690),\Lambda(1690)\to\gamma\Lambda]<5.08\times10^{-7}$, which yields an upper limit of $\mathcal{R}$ for $\Lambda(1690)$ decay of 0.08.

TABLE III. Relative systematic uncertainties (in %) for the branching fraction measurements. Mode I(a) and Mode II(a) correspond to $\Lambda(1520)\to\gamma\Lambda$ and $\Lambda(1520)\to\gamma\Sigma^0$. Mode I(b) and Mode II(b) correspond to $\Lambda(1690)\to\gamma\Lambda$ and $\Lambda(1690)\to\gamma\Sigma^0$, respectively. The items with $*$ are common uncertainties of Mode I(a) and Mode II(a), and the other items are independent uncertainties. In Mode I(b), the additive systematic uncertainties associated with the fitting procedures are excluded as they have already been accounted for in the upper limit described above.

	$\mathcal{R}$			
Source	Mode I(a)	Mode II(a)	Mode I(b)	Mode II(b)
$N_{J/\psi}$	0.4*	0.4*	0.4	0.4
Photon detection	1.0*	2.0*	1.0	2.0
Λ reconstruction	0.7*	0.7*	0.7	0.7
Kinematic fit	3.4*	3.4*	3.4	3.4
Fit range	2.9	1.0	⋯	1.4
Background shape	2.3	4.3	⋯	2.6
$(M^{\rm rec}_{\Lambda\Sigma})^2$	…	1.0	…	3.4
$\chi^2_{\rm 2C}$	…	1.0	…	1.4
$\mathcal{B}(\Lambda\to p\pi)$	1.6*	1.6*	1.6	1.6
Total	6.0		4.0	6.4

Sources of systematic uncertainties and their corresponding contributions to the measurements of the branching fractions are summarized in Table III.

The uncertainty from the total number of J/ψ events, as reported in Ref. [14], is 0.4%. The photon detection efficiency is evaluated using the control sample of $J/\psi\to\rho\pi$ [26], resulting in an uncertainty of 1.0% per photon. Using the clean control sample $J/\psi\to\bar{p}K^+\Lambda$, the momentum-dependent Λ reconstruction efficiency combining the tracking efficiency has been studied in a given $\cos\theta$ range. The difference on efficiency between data and MC simulation is taken as the corresponding systematic uncertainty. The uncertainty associated with the kinematic fit comes from the inconsistency between data and MC simulation of the track parameters and the error matrices. The helix parameters of the charged tracks and their errors of the MC simulation are then corrected to improve the consistency between data and MC simulation [27]; the difference of the signal efficiencies before and after this correction is taken as the systematic uncertainty.

The fitting related uncertainty, including fit range and background shape, is determined by varying the background functions and the fit ranges. This also yields the uncertainties of 0.2 MeV/c^2 and 0.7 MeV for the mass and

width of the $\Lambda(1520)$, and 0.5 MeV/c^2 and 1.2 MeV for those of the $\Lambda(1690)$. Additionally, the potential interference between the $\Lambda(1520)$ resonance and the nonresonant background is considered as an additional systematic uncertainty associated with the fit model. This uncertainty is evaluated by comparing the baseline fit with an alternative fit that includes an interference term. The resulting shifts in the resonance parameters, which are 1.8 MeV/c^2 for the mass and 0.9 MeV for the width of the $\Lambda(1520)$ and 0.4 MeV/c^2 for the mass and 1.0 MeV for the width of the $\Lambda(1690)$, are incorporated into the total systematic uncertainty. The uncertainties arising from the veto of $\Lambda\bar{\Sigma}^0\pi^0$ events are estimated by varying the requirements of $(M^{\rm rec}_{\Lambda\Sigma})^2$ and $\chi^2_{\rm 2C}$. And the maximum changes of the results for $\Lambda(1520) \to \gamma\Sigma^0$ and $\Lambda(1690) \to \gamma\Sigma^0$, respectively, are assigned as the systematic uncertainties.

All of the above contributions and the uncertainty from the branching fraction of $\Lambda \to p\pi^-$ are summarized in Table III, where the total systematic uncertainty is given by the sum in quadrature of the individual errors, assuming that all sources are independent. In the calculation of the total systematic uncertainty of $\mathcal{R}$, the common systematic uncertainties cancel, e.g., the uncertainties associated with the total number of J/ψ events, the Λ reconstruction, the kinematic fit, and the branching fraction of $\Lambda \to p\pi^-$. For the decay $\Lambda(1690) \to \gamma\Lambda$, the additive systematic uncertainties related to the fit procedures are not present in Table III as they have been considered in the determination of the upper limit described above.

In summary, with a sample of 10 billion J/ψ events taken with the BESIII detector, we observe the radiative transition $\Lambda(1520) \to \gamma\Sigma^0$ with a statistical significance of 16.6σ for the first time. The extracted width of $[17.6 \pm 1.6(\text{stat}) \pm 1.1(\text{syst})]$ MeV is consistent with the world average, whereas the mass of the $\Lambda(1520)$ is determined to be $[1515.4 \pm 0.5(\text{stat}) \pm 1.8(\text{syst})]$ MeV/c^2. The ratio of the branching fractions of $\Lambda(1520) \to \gamma\Lambda$ to $\Lambda(1520) \to \gamma\Sigma^0$ is determined to be $3.19 \pm 0.34(\text{stat}) \pm 0.19(\text{syst})$, which is consistent with the prediction of flavor SU(3) [8] within two standard deviations. Consequently, based on the nominal $\mathcal{B}[\Lambda(1520) \to \gamma\Lambda]$ of $(0.85 \pm 0.15)\%$ [21], the branching fraction of $\Lambda(1520) \to \gamma\Sigma^0$ is measured to be $\mathcal{B}[\Lambda(1520) \to \gamma\Sigma^0] = [2.66 \pm 0.28(\text{stat}) \pm 0.50(\text{syst})] \times 10^{-3}$. Based on the fitted width of $\Lambda(1520)$, the radiative width of $\Lambda(1520) \to \gamma\Sigma^0$ is measured to be $[46.8 \pm 6.6(\text{stat}) \pm 9.3(\text{syst})]$ keV. As a result, the significant discrepancies observed with the predictions from both the RCQM [11] and the Algebraic model [13] strongly indicate that these two models are unlikely to serve as suitable representations. However, our measurements of $\Lambda(1520) \to \gamma\Sigma^0$ partial widths, combined with nominal values [21] for $\Lambda(1520) \to \gamma\Lambda$, demonstrate that only NRQM calculations [9] are currently compatible with experimental data. Although there are clear discrepancies between our results and other theoretical models, the limited statistical precision of our data and incomplete uncertainty quantification in the theoretical models currently preclude definitive assessment of their validity.

Moreover, the $\Lambda(1690) \to \gamma\Sigma^0$ decay is observed with a statistical significance of 23.2σ for the first time, and the mass of $[1683.9 \pm 1.3(\text{stat}) \pm 0.6(\text{syst})]$ MeV/c^2 and a width of $[48.8 \pm 4.0(\text{stat}) \pm 1.6(\text{syst})]$ MeV are determined. Furthermore, the product branching fraction is determined to be $\mathcal{B}(J/\psi \to \bar{\Lambda}\Lambda(1690)) \times \mathcal{B}(\Lambda(1690) \to \gamma\Sigma^0) = [6.05 \pm 0.42(\text{stat}) \pm 0.39(\text{syst})] \times 10^{-6}$. Of interest is the absence of this structure in the $\gamma\Lambda$ mass spectrum, and the upper limit on the product branching fraction is $\mathcal{B}(J/\psi \to \bar{\Lambda}\Lambda(1690)) \times \mathcal{B}(\Lambda(1690) \to \gamma\Lambda) < 5.08 \times 10^{-7}$ at the 90% confidence level, and the corresponding ratio of these two decays is determined to be less than 0.08. Currently, no well-established theory explains this phenomenon. One possible explanation is that this resonant structure may actually originate from $\Sigma(1670)$ rather than $\Lambda(1690)$. In this scenario, it is reasonable to expect that the decay of $\Sigma(1670) \to \gamma\Lambda$ is suppressed. However, the decay $J/\psi \to \bar{\Lambda}\Sigma(1670)$ would also be suppressed due to the isospin violation. Given the existing limited statistics, it is challenging to distinguish between the resonant structures of $\Lambda(1690)$ and $\Sigma(1670)$. Since the dominant decay of $\Sigma(1670)$ is $\Sigma(1670) \to \Sigma^0\pi^0$, future investigations utilizing partial wave analysis of $J/\psi \to \bar{\Lambda}\Sigma^0\pi^0$ may provide clearer insights into this issue.

Acknowledgments—The BESIII Collaboration thanks the staff of BEPCII and the IHEP computing center for their strong support. This work is supported in part by National Key R&D Program of China under Contracts No. 2025YFA1613900, No. 2023YFA1606000, and No. 2023YFA1606704; the National Natural Science Foundation of China (NSFC) under Contracts No. 11635010, No. 11935015, No. 11935016, No. 11935018, No. 12025502, No. 12035009, No. 12035013, No. 12061131003, No. 12192260, No. 12192261, No. 12192262, No. 12192263, No. 12192264, No. 12192265, No. 12221005, No. 12225509, No. 12235017, No. 12342502, No. 12361141819, and No. 12475089; the Chinese Academy of Sciences (CAS) Large-Scale Scientific Facility Program; CAS under Contract No. YSBR-101; 100 Talents Program of CAS; The Institute of Nuclear and Particle Physics (INPAC) and Shanghai Key Laboratory for Particle Physics and Cosmology; German Research Foundation DFG under Contract No. FOR5327; Istituto Nazionale di Fisica Nucleare, Italy; Knut and Alice Wallenberg Foundation under Contracts No. 2021.0174 and No. 2021.0299; Ministry of Development of Turkey under Contract No. DPT2006K-120470; National Research Foundation of Korea under Contract No. NRF-2022R1A2C1092335; National Science and Technology fund of Mongolia; Polish National Science Centre under Contract No. 2024/53/B/ST2/00975; Swedish Research

Council under Contract No. 2019.04595; and U.S. Department of Energy under Contract No. DE-FG02-05ER41374.

Data availability—The data that support the findings of this article are not publicly available. The data are available from the authors upon reasonable request.

[1] R. Bertini, Nucl. Phys. **B279**, 49 (1987).
[2] N. Isgur and G. Karl, Phys. Rev. D **18**, 4187 (1978).
[3] N. Isgur and G. Karl, Phys. Rev. D **20**, 1191 (1979).
[4] L. Yu, X. L. Chen, W. Z. Deng, and S. L. Zhu, Phys. Rev. D **73**, 114001 (2006).
[5] M. Ablikim *et al.* (BESIII Collaboration), Phys. Rev. Lett. **130**, 211901 (2023).
[6] M. Ablikim *et al.* (BESIII Collaboration), Phys. Rev. Lett. **129**, 212002 (2022).
[7] S. Taylor *et al.* (CLAS Collaboration), Phys. Rev. C **71**, 054609 (2005).
[8] L. G. Landsberg, Phys. At. Nucl. **59**, 2080 (1996).
[9] E. Kaxiras, E. J. Moniz, and M. Soyeur, Phys. Rev. D **32**, 695 (1985).
[10] J. W. Darewych, M. Horbatsch, and R. Koniuk, Phys. Rev. D **28**, 1125 (1983).
[11] M. Warns, W. Pfeil, and H. Rollnik, Phys. Lett. B **258**, 431 (1991).
[12] Y. Umino and F. Myhrer, Nucl. Phys. **A529**, 713 (1991).
[13] R. Bijker, F. Iachello, and A. Leviatan, Ann. Phys. (N.Y.) **284**, 89 (2000).
[14] M. Ablikim *et al.* (BESIII Collaboration), Chin. Phys. C **46**, 074001 (2022).
[15] M. Ablikim *et al.* (BESIII Collaboration), Nucl. Instrum. Methods Phys. Res., Sect. A **614**, 345 (2010).
[16] M. Ablikim *et al.* (BESIII Collaboration), Chin. Phys. C **44**, 040001 (2020).
[17] S. Agostinelli *et al.* (GEANT4 Collaboration), Nucl. Instrum. Methods Phys. Res., Sect. A **506**, 250 (2003).
[18] D. J. Lange, Nucl. Instrum. Methods Phys. Res., Sect. A **462**, 152 (2001).
[19] R. G. Ping, Chin. Phys. C **32**, 599 (2008).
[20] M. Xu *et al.*, Chin. Phys. C **33**, 428 (2009).
[21] S. Navas *et al.* (Particle Data Group), Phys. Rev. D **110**, 030001 (2024).
[22] J. C. Chen, G. S. Huang, X. R. Qi, D. H. Zhang, and Y. S. Zhu, Phys. Rev. D **62**, 034003 (2000).
[23] R. L. Yang, R. G. Ping, and H. Chen, Chin. Phys. Lett. **31**, 061301 (2014).
[24] See Supplemental Material at http://link.aps.org/supplemental/10.1103/l6g2-2wg6 for the data-driven sideband analysis and the helicity amplitude analysis of $\Lambda(1690)$ assignment.
[25] Y. S. Zhu, Chin. Phys. C **32**, 363 (2008).
[26] M. Ablikim *et al.* (BESIII Collaboration), Phys. Rev. D **83**, 112005 (2011).
[27] M. Ablikim *et al.* (BESIII Collaboration), Phys. Rev. D **87**, 012002 (2013).

M. Ablikim,[1] M. N. Achasov,[4,c] P. Adlarson,[77] X. C. Ai,[82] R. Aliberti,[36] A. Amoroso,[76a,76c] Q. An,[59,73,a] Y. Bai,[58] O. Bakina,[37] Y. Ban,[47,h] H.-R. Bao,[65] V. Batozskaya,[1,45] K. Begzsuren,[33] N. Berger,[36] M. Berlowski,[45] M. Bertani,[29a] D. Bettoni,[30a] F. Bianchi,[76a,76c] E. Bianco,[76a,76c] A. Bortone,[76a,76c] I. Boyko,[37] R. A. Briere,[5] A. Brueggemann,[70] H. Cai,[78] M. H. Cai,[39,k,l] X. Cai,[1,59] A. Calcaterra,[29a] G. F. Cao,[1,65] N. Cao,[1,65] S. A. Cetin,[63a] X. Y. Chai,[47,h] J. F. Chang,[1,59] G. R. Che,[44] Y. Z. Che,[1,59,65] C. H. Chen,[9] Chao Chen,[56] G. Chen,[1] H. S. Chen,[1,65] H. Y. Chen,[21] M. L. Chen,[1,59,65] S. J. Chen,[43] S. L. Chen,[46] S. M. Chen,[62] T. Chen,[1,65] X. R. Chen,[32,65] X. T. Chen,[1,65] X. Y. Chen,[12,g] Y. B. Chen,[1,59] Y. Q. Chen,[35] Y. Q. Chen,[16] Z. Chen,[25] Z. J. Chen,[26,i] Z. K. Chen,[60] S. K. Choi,[10] X. Chu,[12,g] G. Cibinetto,[30a] F. Cossio,[76c] J. Cottee-Meldrum,[64] J. J. Cui,[51] H. L. Dai,[1,59] J. P. Dai,[80] A. Dbeyssi,[19] R. E. de Boer,[3] D. Dedovich,[37] C. Q. Deng,[74] Z. Y. Deng,[1] A. Denig,[36] I. Denysenko,[37] M. Destefanis,[76a,76c] F. De Mori,[76a,76c] B. Ding,[1,68] X. X. Ding,[47,h] Y. Ding,[41] Y. Ding,[35] Y. X. Ding,[31] J. Dong,[1,59] L. Y. Dong,[1,65] M. Y. Dong,[1,59,65] X. Dong,[78] M. C. Du,[1] S. X. Du,[82] S. X. Du,[12,g] Y. Y. Duan,[56] P. Egorov,[37,b] G. F. Fan,[43] J. J. Fan,[20] Y. H. Fan,[46] J. Fang,[1,59] J. Fang,[60] S. S. Fang,[1,65] W. X. Fang,[1] Y. Q. Fang,[1,59] R. Farinelli,[30a] L. Fava,[76b,76c] F. Feldbauer,[3] G. Felici,[29a] C. Q. Feng,[59,73] J. H. Feng,[16] L. Feng,[39,k,l] Q. X. Feng,[39,k,l] Y. T. Feng,[59,73] M. Fritsch,[3] C. D. Fu,[1] J. L. Fu,[65] Y. W. Fu,[1,65] H. Gao,[65] X. B. Gao,[42] Y. Gao,[59,73] Y. N. Gao,[47,h] Y. N. Gao,[20] Y. Y. Gao,[31] S. Garbolino,[76c] I. Garzia,[30a,30b] P. T. Ge,[20] Z. W. Ge,[43] C. Geng,[60] E. M. Gersabeck,[69] A. Gilman,[71] K. Goetzen,[13] J. D. Gong,[35] L. Gong,[41] W. X. Gong,[1,59] W. Gradl,[36] S. Gramigna,[30a,30b] M. Greco,[76a,76c] M. H. Gu,[1,59] Y. T. Gu,[15] C. Y. Guan,[1,65] A. Q. Guo,[32] L. B. Guo,[42] M. J. Guo,[51] R. P. Guo,[50] Y. P. Guo,[12,g] A. Guskov,[37,b] J. Gutierrez,[28] K. L. Han,[65] T. T. Han,[1] F. Hanisch,[3] K. D. Hao,[59,73] X. Q. Hao,[20] F. A. Harris,[67] K. K. He,[56] K. L. He,[1,65] F. H. Heinsius,[3] C. H. Heinz,[36] Y. K. Heng,[1,59,65] C. Herold,[61] P. C. Hong,[35] G. Y. Hou,[1,65] X. T. Hou,[1,65] Y. R. Hou,[65] Z. L. Hou,[1] H. M. Hu,[1,65] J. F. Hu,[57,j] Q. P. Hu,[59,73] S. L. Hu,[12,g] T. Hu,[1,59,65] Y. Hu,[1] Z. M. Hu,[60] G. S. Huang,[59,73] K. X. Huang,[60] L. Q. Huang,[32,65] P. Huang,[43] X. T. Huang,[51]

Y. P. Huang,[1] Y. S. Huang,[60] T. Hussain,[75] N. Hüsken,[36] N. in der Wiesche,[70] J. Jackson,[28] Q. Ji,[1] Q. P. Ji,[20] W. Ji,[1,65] X. B. Ji,[1,65] X. L. Ji,[1,59] Y. Y. Ji,[51] Z. K. Jia,[59,73] D. Jiang,[1,65] H. B. Jiang,[78] P. C. Jiang,[47,h] S. J. Jiang,[9] T. J. Jiang,[17] X. S. Jiang,[1,59,65] Y. Jiang,[65] J. B. Jiao,[51] J. K. Jiao,[35] Z. Jiao,[24] S. Jin,[43] Y. Jin,[68] M. Q. Jing,[1,65] X. M. Jing,[65] T. Johansson,[77] S. Kabana,[34] N. Kalantar-Nayestanaki,[66] X. L. Kang,[9] X. S. Kang,[41] M. Kavatsyuk,[66] B. C. Ke,[82] V. Khachatryan,[28] A. Khoukaz,[70] R. Kiuchi,[1] O. B. Kolcu,[63a] B. Kopf,[3] M. Kuessner,[3] X. Kui,[1,65] N. Kumar,[27] A. Kupsc,[45,77] W. Kühn,[38] Q. Lan,[74] W. N. Lan,[20] T. T. Lei,[59,73] M. Lellmann,[36] T. Lenz,[36] C. Li,[59,73] C. Li,[48] C. Li,[44] C. H. Li,[40] C. K. Li,[21] D. M. Li,[82] F. Li,[1,59] G. Li,[1] H. B. Li,[1,65] H. J. Li,[20] H. N. Li,[57,j] Hui Li,[44] J. R. Li,[62] J. S. Li,[60] K. Li,[1] K. L. Li,[20] K. L. Li,[39,k,l] L. J. Li,[1,65] Lei Li,[49] M. H. Li,[44] M. R. Li,[1,65] P. L. Li,[65] P. R. Li,[39,k,l] Q. M. Li,[1,65] Q. X. Li,[51] R. Li,[18,32] S. X. Li,[12] T. Li,[51] T. Y. Li,[44] W. D. Li,[1,65] W. G. Li,[1,a] X. Li,[1,65] X. H. Li,[59,73] X. L. Li,[51] X. Y. Li,[1,8] X. Z. Li,[60] Y. Li,[20] Y. G. Li,[47,h] Y. P. Li,[35] Z. J. Li,[60] Z. Y. Li,[80] H. Liang,[59,73] Y. F. Liang,[55] Y. T. Liang,[32,65] G. R. Liao,[14] L. B. Liao,[60] M. H. Liao,[60] Y. P. Liao,[1,65] J. Libby,[27] A. Limphirat,[61] C. C. Lin,[56] D. X. Lin,[32,65] L. Q. Lin,[40] T. Lin,[1] B. J. Liu,[1] B. X. Liu,[78] C. Liu,[35] C. X. Liu,[1] F. Liu,[1] F. H. Liu,[54] Feng Liu,[6] G. M. Liu,[57,j] H. Liu,[39,k,l] H. B. Liu,[15] H. H. Liu,[1] H. M. Liu,[1,65] Huihui Liu,[22] J. B. Liu,[59,73] J. J. Liu,[21] K. Liu,[39,k,l] K. Liu,[74] K. Y. Liu,[41] Ke Liu,[23] L. C. Liu,[44] Lu Liu,[44] M. H. Liu,[12,g] P. L. Liu,[1] Q. Liu,[65] S. B. Liu,[59,73] T. Liu,[12,g] W. K. Liu,[44] W. M. Liu,[59,73] W. T. Liu,[40] X. Liu,[39,k,l] X. Liu,[40] X. K. Liu,[39,k,l] X. Y. Liu,[78] Y. Liu,[39,k,l] Y. Liu,[82] Yuan Liu,[82] Y. B. Liu,[44] Z. A. Liu,[1,59,65] Z. D. Liu,[9] Z. Q. Liu,[51] X. C. Lou,[1,59,65] F. X. Lu,[60] H. J. Lu,[24] J. G. Lu,[1,59] X. L. Lu,[16] Y. Lu,[7] Y. H. Lu,[1,65] Y. P. Lu,[1,59] Z. H. Lu,[1,65] C. L. Luo,[42] J. R. Luo,[60] J. S. Luo,[1,65] M. X. Luo,[81] T. Luo,[12,g] X. L. Luo,[1,59] Z. Y. Lv,[23] X. R. Lyu,[65,p] Y. F. Lyu,[44] Y. H. Lyu,[82] F. C. Ma,[41] H. L. Ma,[1] J. L. Ma,[1,65] L. L. Ma,[51] L. R. Ma,[68] Q. M. Ma,[1] R. Q. Ma,[1,65] R. Y. Ma,[20] T. Ma,[59,73] X. T. Ma,[1,65] X. Y. Ma,[1,59] Y. M. Ma,[32] F. E. Maas,[19] I. MacKay,[71] M. Maggiora,[76a,76c] S. Malde,[71] Q. A. Malik,[75] H. X. Mao,[39,k,l] Y. J. Mao,[47,h] Z. P. Mao,[1] S. Marcello,[76a,76c] A. Marshall,[64] F. M. Melendi,[30a,30b] Y. H. Meng,[65] Z. X. Meng,[68] G. Mezzadri,[30a] H. Miao,[1,65] T. J. Min,[43] R. E. Mitchell,[28] X. H. Mo,[1,59,65] B. Moses,[28] N. Yu. Muchnoi,[4,c] J. Muskalla,[36] Y. Nefedov,[37] F. Nerling,[19,e] L. S. Nie,[21] I. B. Nikolaev,[4,c] Z. Ning,[1,59] S. Nisar,[11,m] Q. L. Niu,[39,k,l] W. D. Niu,[12,g] C. Normand,[64] S. L. Olsen,[10,65] Q. Ouyang,[1,59,65] S. Pacetti,[29b,29c] X. Pan,[56] Y. Pan,[58] A. Pathak,[10] Y. P. Pei,[59,73] M. Pelizaeus,[3] H. P. Peng,[59,73] X. J. Peng,[39,k,l] Y. Y. Peng,[39,k,l] K. Peters,[13,e] K. Petridis,[64] J. L. Ping,[42] R. G. Ping,[1,65] S. Plura,[36] V. Prasad,[35] F. Z. Qi,[1] H. R. Qi,[62] M. Qi,[43] S. Qian,[1,59] W. B. Qian,[65] C. F. Qiao,[65] J. H. Qiao,[20] J. J. Qin,[74] J. L. Qin,[56] L. Q. Qin,[14] L. Y. Qin,[59,73] P. B. Qin,[74] X. P. Qin,[12,g] X. S. Qin,[51] Z. H. Qin,[1,59] J. F. Qiu,[1] Z. H. Qu,[74] J. Rademacker,[64] C. F. Redmer,[36] A. Rivetti,[76c] M. Rolo,[76c] G. Rong,[1,65] S. S. Rong,[1,65] F. Rosini,[29b,29c] Ch. Rosner,[19] M. Q. Ruan,[1,59] N. Salone,[45] A. Sarantsev,[37,d] Y. Schelhaas,[36] K. Schoenning,[77] M. Scodeggio,[30a] K. Y. Shan,[12,g] W. Shan,[25] X. Y. Shan,[59,73] Z. J. Shang,[39,k,l] J. F. Shangguan,[17] L. G. Shao,[1,65] M. Shao,[59,73] C. P. Shen,[12,g] H. F. Shen,[1,8] W. H. Shen,[65] X. Y. Shen,[1,65] B. A. Shi,[65] H. Shi,[59,73] J. L. Shi,[12,g] J. Y. Shi,[1] S. Y. Shi,[74] X. Shi,[1,59] H. L. Song,[59,73] J. J. Song,[20] T. Z. Song,[60] W. M. Song,[35] Y. J. Song,[12,g] Y. X. Song,[47,h,n] S. Sosio,[76a,76c] S. Spataro,[76a,76c] F. Stieler,[36] S. S. Su,[41] Y. J. Su,[65] G. B. Sun,[78] G. X. Sun,[1] H. Sun,[65] H. K. Sun,[1] J. F. Sun,[20] K. Sun,[62] L. Sun,[78] S. S. Sun,[1,65] T. Sun,[52,f] Y. C. Sun,[78] Y. H. Sun,[31] Y. J. Sun,[59,73] Y. Z. Sun,[1] Z. Q. Sun,[1,65] Z. T. Sun,[51] C. J. Tang,[55] G. Y. Tang,[1] J. Tang,[60] J. J. Tang,[59,73] L. F. Tang,[40] Y. A. Tang,[78] L. Y. Tao,[74] M. Tat,[71] J. X. Teng,[59,73] J. Y. Tian,[59,73] W. H. Tian,[60] Y. Tian,[32] Z. F. Tian,[78] I. Uman,[63b] B. Wang,[1] B. Wang,[60] Bo Wang,[59,73] C. Wang,[39,k,l] C. Wang,[20] Cong Wang,[23] D. Y. Wang,[47,h] H. J. Wang,[39,k,l] J. J. Wang,[78] K. Wang,[1,59] L. L. Wang,[1] L. W. Wang,[35] M. Wang,[51] M. Wang,[59,73] N. Y. Wang,[65] S. Wang,[12,g] T. Wang,[12,g] T. J. Wang,[44] W. Wang,[60] Wei Wang,[74] W. P. Wang,[36,59,73,o] X. Wang,[47,h] X. F. Wang,[39,k,l] X. J. Wang,[40] X. L. Wang,[12,g] X. N. Wang,[1] Y. Wang,[62] Y. D. Wang,[46] Y. F. Wang,[1,8,65] Y. H. Wang,[39,k,l] Y. J. Wang,[59,73] Y. L. Wang,[20] Y. N. Wang,[78] Y. Q. Wang,[1] Yaqian Wang,[18] Yi Wang,[62] Yuan Wang,[18,32] Z. Wang,[1,59] Z. L. Wang,[74] Z. L. Wang,[2] Z. Q. Wang,[12,g] Z. Y. Wang,[1,65] D. H. Wei,[14] H. R. Wei,[44] F. Weidner,[70] S. P. Wen,[1] Y. R. Wen,[40] U. Wiedner,[3] G. Wilkinson,[71] M. Wolke,[77] C. Wu,[40] J. F. Wu,[1,8] L. H. Wu,[1] L. J. Wu,[1,65] L. J. Wu,[20] Lianjie Wu,[20] S. G. Wu,[1,65] S. M. Wu,[65] X. Wu,[12,g] X. H. Wu,[35] Y. J. Wu,[32] Z. Wu,[1,59] L. Xia,[59,73] X. M. Xian,[40] B. H. Xiang,[1,65] D. Xiao,[39,k,l] G. Y. Xiao,[43] H. Xiao,[74] Y. L. Xiao,[12,g] Z. J. Xiao,[42] C. Xie,[43] K. J. Xie,[1,65] X. H. Xie,[47,h] Y. Xie,[51] Y. G. Xie,[1,59] Y. H. Xie,[6] Z. P. Xie,[59,73] T. Y. Xing,[1,65] C. F. Xu,[1,65]

C. J. Xu,[60] G. F. Xu,[1] H. Y. Xu,[2,68] H. Y. Xu,[2] M. Xu,[59,73] Q. J. Xu,[17] Q. N. Xu,[31] T. D. Xu,[74] W. Xu,[1] W. L. Xu,[68] X. P. Xu,[56] Y. Xu,[41] Y. Xu,[12,g] Y. C. Xu,[79] Z. S. Xu,[65] F. Yan,[12,g] H. Y. Yan,[40] L. Yan,[12,g] W. B. Yan,[59,73] W. C. Yan,[82] W. H. Yan,[6] W. P. Yan,[20] X. Q. Yan,[1,65] H. J. Yang,[52,f] H. L. Yang,[35] H. X. Yang,[1] J. H. Yang,[43] R. J. Yang,[20] T. Yang,[1] Y. Yang,[12,g] Y. F. Yang,[44] Y. H. Yang,[43] Y. Q. Yang,[9] Y. X. Yang,[1,65] Y. Z. Yang,[20] M. Ye,[1,59] M. H. Ye,[8,a] Z. J. Ye,[57,j] Junhao Yin,[44] Z. Y. You,[60] B. X. Yu,[1,59,65] C. X. Yu,[44] G. Yu,[13] J. S. Yu,[26,i] L. Q. Yu,[12,g] M. C. Yu,[41] T. Yu,[74] X. D. Yu,[47,h] Y. C. Yu,[82] C. Z. Yuan,[1,65] H. Yuan,[1,65] J. Yuan,[35] J. Yuan,[46] L. Yuan,[2] S. C. Yuan,[1,65] X. Q. Yuan,[1] Y. Yuan,[1,65] Z. Y. Yuan,[60] C. X. Yue,[40] Ying Yue,[20] A. A. Zafar,[75] S. H. Zeng,[64] X. Zeng,[12,g] Y. Zeng,[26,i] Yujie Zeng,[60] Y. J. Zeng,[1,65] X. Y. Zhai,[35] Y. H. Zhan,[60] A. Q. Zhang,[1,65] B. L. Zhang,[1,65] B. X. Zhang,[1] D. H. Zhang,[44] G. Y. Zhang,[20] G. Y. Zhang,[1,65] H. Zhang,[59,73] H. Zhang,[82] H. C. Zhang,[1,59,65] H. H. Zhang,[60] H. Q. Zhang,[1,59,65] H. R. Zhang,[59,73] H. Y. Zhang,[1,59] Jin Zhang,[82] J. Zhang,[60] J. J. Zhang,[53] J. L. Zhang,[21] J. Q. Zhang,[42] J. S. Zhang,[12,g] J. W. Zhang,[1,59,65] J. X. Zhang,[39,k,l] J. Y. Zhang,[1] J. Z. Zhang,[1,65] Jianyu Zhang,[65] L. M. Zhang,[62] Lei Zhang,[43] N. Zhang,[82] P. Zhang,[1,8] Q. Zhang,[20] Q. Y. Zhang,[35] R. Y. Zhang,[39,k,l] S. H. Zhang,[1,65] Shulei Zhang,[26,i] X. M. Zhang,[1] X. Y. Zhang,[41] X. Y. Zhang,[51] Y. Zhang,[1] Y. Zhang,[74] Y. T. Zhang,[82] Y. H. Zhang,[1,59] Y. M. Zhang,[40] Y. P. Zhang,[59,73] Z. D. Zhang,[1] Z. H. Zhang,[1] Z. L. Zhang,[35] Z. L. Zhang,[56] Z. X. Zhang,[20] Z. Y. Zhang,[78] Z. Y. Zhang,[44] Z. Z. Zhang,[46] Zh. Zh. Zhang,[20] G. Zhao,[1] J. Y. Zhao,[1,65] J. Z. Zhao,[1,59] L. Zhao,[1] L. Zhao,[59,73] M. G. Zhao,[44] N. Zhao,[80] R. P. Zhao,[65] S. J. Zhao,[82] Y. B. Zhao,[1,59] Y. L. Zhao,[56] Y. X. Zhao,[32,65] Z. G. Zhao,[59,73] A. Zhemchugov,[37,b] B. Zheng,[74] B. M. Zheng,[35] J. P. Zheng,[1,59] W. J. Zheng,[1,8] X. R. Zheng,[20] Y. H. Zheng,[65,p] B. Zhong,[42] C. Zhong,[20] H. Zhou,[36,51,o] J. Q. Zhou,[35] J. Y. Zhou,[35] S. Zhou,[6] X. Zhou,[78] X. K. Zhou,[6] X. R. Zhou,[59,73] X. Y. Zhou,[40] Y. X. Zhou,[79] Y. Z. Zhou,[12,g] A. N. Zhu,[65] J. Zhu,[44] K. Zhu,[1] K. J. Zhu,[1,59,65] K. S. Zhu,[12,g] L. Zhu,[35] L. X. Zhu,[65] S. H. Zhu,[72] T. J. Zhu,[12,g] W. D. Zhu,[42] W. D. Zhu,[12,g] W. J. Zhu,[1] W. Z. Zhu,[20] Y. C. Zhu,[59,73] Z. A. Zhu,[1,65] X. Y. Zhuang,[44] J. H. Zou,[1] and J. Zu[59,73]

(BESIII Collaboration)

[1]*Institute of High Energy Physics, Beijing 100049, People's Republic of China*
[2]*Beihang University, Beijing 100191, People's Republic of China*
[3]*Bochum Ruhr-University, D-44780 Bochum, Germany*
[4]*Budker Institute of Nuclear Physics SB RAS (BINP), Novosibirsk 630090, Russia*
[5]*Carnegie Mellon University, Pittsburgh, Pennsylvania 15213, USA*
[6]*Central China Normal University, Wuhan 430079, People's Republic of China*
[7]*Central South University, Changsha 410083, People's Republic of China*
[8]*China Center of Advanced Science and Technology, Beijing 100190, People's Republic of China*
[9]*China University of Geosciences, Wuhan 430074, People's Republic of China*
[10]*Chung-Ang University, Seoul, 06974, Republic of Korea*
[11]*COMSATS University Islamabad, Lahore Campus, Defence Road, Off Raiwind Road, 54000 Lahore, Pakistan*
[12]*Fudan University, Shanghai 200433, People's Republic of China*
[13]*GSI Helmholtzcentre for Heavy Ion Research GmbH, D-64291 Darmstadt, Germany*
[14]*Guangxi Normal University, Guilin 541004, People's Republic of China*
[15]*Guangxi University, Nanning 530004, People's Republic of China*
[16]*Guangxi University of Science and Technology, Liuzhou 545006, People's Republic of China*
[17]*Hangzhou Normal University, Hangzhou 310036, People's Republic of China*
[18]*Hebei University, Baoding 071002, People's Republic of China*
[19]*Helmholtz Institute Mainz, Staudinger Weg 18, D-55099 Mainz, Germany*
[20]*Henan Normal University, Xinxiang 453007, People's Republic of China*
[21]*Henan University, Kaifeng 475004, People's Republic of China*
[22]*Henan University of Science and Technology, Luoyang 471003, People's Republic of China*
[23]*Henan University of Technology, Zhengzhou 450001, People's Republic of China*
[24]*Huangshan College, Huangshan 245000, People's Republic of China*
[25]*Hunan Normal University, Changsha 410081, People's Republic of China*
[26]*Hunan University, Changsha 410082, People's Republic of China*
[27]*Indian Institute of Technology Madras, Chennai 600036, India*
[28]*Indiana University, Bloomington, Indiana 47405, USA*
[29a]*INFN Laboratori Nazionali di Frascati, INFN Laboratori Nazionali di Frascati, I-00044, Frascati, Italy*

[29b]INFN Sezione di Perugia, I-06100, Perugia, Italy
[29c]University of Perugia, I-06100, Perugia, Italy
[30a]INFN Sezione di Ferrara, INFN Sezione di Ferrara, I-44122, Ferrara, Italy
[30b]University of Ferrara, I-44122, Ferrara, Italy
[31]Inner Mongolia University, Hohhot 010021, People's Republic of China
[32]Institute of Modern Physics, Lanzhou 730000, People's Republic of China
[33]Institute of Physics and Technology, Mongolian Academy of Sciences, Peace Avenue 54B, Ulaanbaatar 13330, Mongolia
[34]Instituto de Alta Investigación, Universidad de Tarapacá, Casilla 7D, Arica 1000000, Chile
[35]Jilin University, Changchun 130012, People's Republic of China
[36]Johannes Gutenberg University of Mainz, Johann-Joachim-Becher-Weg 45, D-55099 Mainz, Germany
[37]Joint Institute for Nuclear Research, 141980 Dubna, Moscow region, Russia
[38]Justus-Liebig-Universitaet Giessen, II. Physikalisches Institut, Heinrich-Buff-Ring 16, D-35392 Giessen, Germany
[39]Lanzhou University, Lanzhou 730000, People's Republic of China
[40]Liaoning Normal University, Dalian 116029, People's Republic of China
[41]Liaoning University, Shenyang 110036, People's Republic of China
[42]Nanjing Normal University, Nanjing 210023, People's Republic of China
[43]Nanjing University, Nanjing 210093, People's Republic of China
[44]Nankai University, Tianjin 300071, People's Republic of China
[45]National Centre for Nuclear Research, Warsaw 02-093, Poland
[46]North China Electric Power University, Beijing 102206, People's Republic of China
[47]Peking University, Beijing 100871, People's Republic of China
[48]Qufu Normal University, Qufu 273165, People's Republic of China
[49]Renmin University of China, Beijing 100872, People's Republic of China
[50]Shandong Normal University, Jinan 250014, People's Republic of China
[51]Shandong University, Jinan 250100, People's Republic of China
[52]Shanghai Jiao Tong University, Shanghai 200240, People's Republic of China
[53]Shanxi Normal University, Linfen 041004, People's Republic of China
[54]Shanxi University, Taiyuan 030006, People's Republic of China
[55]Sichuan University, Chengdu 610064, People's Republic of China
[56]Soochow University, Suzhou 215006, People's Republic of China
[57]South China Normal University, Guangzhou 510006, People's Republic of China
[58]Southeast University, Nanjing 211100, People's Republic of China
[59]State Key Laboratory of Particle Detection and Electronics, Beijing 100049, Hefei 230026, People's Republic of China
[60]Sun Yat-Sen University, Guangzhou 510275, People's Republic of China
[61]Suranaree University of Technology, University Avenue 111, Nakhon Ratchasima 30000, Thailand
[62]Tsinghua University, Beijing 100084, People's Republic of China
[63a]Turkish Accelerator Center Particle Factory Group, Istinye University, 34010, Istanbul, Turkey
[63b]Near East University, Nicosia, North Cyprus, 99138, Mersin 10, Turkey
[64]University of Bristol, H H Wills Physics Laboratory, Tyndall Avenue, Bristol, BS8 1TL, United Kingdom
[65]University of Chinese Academy of Sciences, Beijing 100049, People's Republic of China
[66]University of Groningen, NL-9747 AA Groningen, The Netherlands
[67]University of Hawaii, Honolulu, Hawaii 96822, USA
[68]University of Jinan, Jinan 250022, People's Republic of China
[69]University of Manchester, Oxford Road, Manchester, M13 9PL, United Kingdom
[70]University of Muenster, Wilhelm-Klemm-Strasse 9, 48149 Muenster, Germany
[71]University of Oxford, Keble Road, Oxford OX13RH, United Kingdom
[72]University of Science and Technology Liaoning, Anshan 114051, People's Republic of China
[73]University of Science and Technology of China, Hefei 230026, People's Republic of China
[74]University of South China, Hengyang 421001, People's Republic of China
[75]University of the Punjab, Lahore-54590, Pakistan
[76a]University of Turin and INFN, University of Turin, I-10125, Turin, Italy
[76b]University of Eastern Piedmont, I-15121, Alessandria, Italy
[76c]INFN, I-10125, Turin, Italy
[77]Uppsala University, Box 516, SE-75120 Uppsala, Sweden
[78]Wuhan University, Wuhan 430072, People's Republic of China
[79]Yantai University, Yantai 264005, People's Republic of China
[80]Yunnan University, Kunming 650500, People's Republic of China
[81]Zhejiang University, Hangzhou 310027, People's Republic of China
[82]Zhengzhou University, Zhengzhou 450001, People's Republic of China

[a]Deceased.
[b]Also at the Moscow Institute of Physics and Technology, Moscow 141700, Russia.
[c]Also at the Novosibirsk State University, Novosibirsk, 630090, Russia.
[d]Also at the NRC "Kurchatov Institute," PNPI, 188300, Gatchina, Russia.
[e]Also at Goethe University Frankfurt, 60323 Frankfurt am Main, Germany.
[f]Also at Key Laboratory for Particle Physics, Astrophysics and Cosmology, Ministry of Education; Shanghai Key Laboratory for Particle Physics and Cosmology; Institute of Nuclear and Particle Physics, Shanghai 200240, People's Republic of China.
[g]Also at Key Laboratory of Nuclear Physics and Ion-beam Application (MOE) and Institute of Modern Physics, Fudan University, Shanghai 200443, People's Republic of China.
[h]Also at State Key Laboratory of Nuclear Physics and Technology, Peking University, Beijing 100871, People's Republic of China.
[i]Also at School of Physics and Electronics, Hunan University, Changsha 410082, China.
[j]Also at Guangdong Provincial Key Laboratory of Nuclear Science, Institute of Quantum Matter, South China Normal University, Guangzhou 510006, China.
[k]Also at MOE Frontiers Science Center for Rare Isotopes, Lanzhou University, Lanzhou 730000, People's Republic of China.
[l]Also at Lanzhou Center for Theoretical Physics, Lanzhou University, Lanzhou 730000, People's Republic of China.
[m]Also at the Department of Mathematical Sciences, IBA, Karachi 75270, Pakistan.
[n]Also at Ecole Polytechnique Federale de Lausanne (EPFL), CH-1015 Lausanne, Switzerland.
[o]Also at Helmholtz Institute Mainz, Staudinger Weg 18, D-55099 Mainz, Germany.
[p]Also at Hangzhou Institute for Advanced Study, University of Chinese Academy of Sciences, Hangzhou 310024, China.